ISSN (online): 3008-0436 ISSN (print): 3008-0428

Aquatic Resource Sciences

Journal homepage: www.journal.inrrd.com/ars

Original article

Temporal Land Use Change Pattern of Kaptai Lake and Surrounding Area Using Remotely Sensed Data

Md. Al-Amin[1], Md. Mujibor Rahman[1]*, Kamrun Nahar[2], Raqibul Islam[2], Ahsan Imam[1] and Md Kamrul Haque[3]

[1]*Environmental Science Discipline, Khulna University, Khulna 9208, Bangladesh*
[2]*School of Management, Kettering University, Flint, Michigan 48504, USA*
[3]*Institute of Natural Resources Research & Development, Rajshahi 6206, Bangladesh*

ARTICLE INFO

Article history
Received 27 March 2025
Revised 08 June 2025
Accepted 21 June 2025
Available online 30 June 2025

Keywords
Kaptai lake
Temporal land use change
Water level change
LULC
NDVI
Remote Sensing
GIS

ABSTRACT

Kaptai lake and its surrounding area have become a very important place due to its natural resources, which generate a significant share of Bangladesh's power supply using hydropower. Over the past few decades, water level and forest cover depletion have become major problems because of human intervention. Studies have been performed to assess the changes in water level, land cover, vegetation health, and surface temperature in this area. To perform "change detection" on Landsat satellite images, those from 1976, 1989, 2005, and 2018 have been used. Three land cover classes were used via "regions of interest" to perform the "maximum likelihood" algorithm of the supervised classification system. Over the past 42 years, land cover analysis reveals a decrease in water bodies from 10.48% in 1976 to 9.55% in 2018. In contrast, paved surfaces increased from 10.66% in 1976 to 24.28% in 2018, while vegetation cover declined from 79.80% to 65.23% over the same period. Normalized Difference Vegetation Index (NDVI) values were extracted using ENVI Classic 5.3 remote sensing software to generate NDVI maps. The study shows that, over the past 29 years, vegetation health categories have changed significantly: sparse vegetation increased from 13.04% in 1989 to 19.32% in 2018; moderate vegetation from 13.04% to 19.83%; while dense vegetation declined sharply from 47.83% to 21.36%, indicating a significant deterioration in vegetation health in the Kaptai sub-basin. Further, the study illustrates that last 29 years' change of maximum temperature, which indicates paved surface temperature, is increased greatly from 26.25 ^{0}C in 1989 to 29.59 ^{0}C in 2018, while minimum temperature, which indicate vegetation cover temperature, is increased in little rate from 16.10 ^{0}C in 1989 to 17.48 ^{0}C in 2018, respectively. This study is a preliminary effort to look into the land cover change pattern of Kaptai sub-basin, which might be useful as a starting point for further in-depth spatial studies of these problems to figure out potential solutions.

Introduction

Man-made lakes affect the environment in many ways. Some of these effects include landscape and land-use/land-cover changes, loss of habitat for existing species due to flooding, and the settlement of new inhabitants in the flooded area (Dale et al. 2011). They can also alter groundwater levels, potentially leading to the decline of ambient species sensitive to such disturbances (Antonić et al. 2001). Kaptai lake is one of the most important freshwater bodies and is the largest man-made freshwater resource in Southeast Asia as well as in Bangladesh (Tripura 2021). This lake, a sub-basin of the Karnaphuli River, was primarily created for hydroelectric power generation. Although its primary purpose was hydroelectricity, Kaptai lake now also significantly contributes to freshwater fish production, flood control, tourism, and agriculture. Recent assessments of the lake's ecological condition have revealed that water pollution is caused by fertilizers and pesticides used in nearby agricultural fields, which contaminate the lake water (Das et al. 2024). Forest depletion and reservoir sedimentation have become serious issues in the lake area

*Corresponding author
Email address: mujibku@gmail.com (Md. Mujibor Rahman)

(Suman et al. 2021). The replacement of forest cover with shifting cultivation has led to increased soil erosion, contributing large amounts of sediment to the reservoir and posing serious threats to both the power plant and navigability (Salehin 2024). With advancements in technology, decreasing data costs, the availability of historical spatio-temporal data, and high-resolution satellite imagery, GIS and remote sensing techniques have become valuable tools for land cover change detection and future scenario prediction (Seyam et al. 2023).

Temporal land-use change patterns result from complex interactions between human activities and the physical environment (Li and Hao 2003). Satellite-based Earth observation and monitoring provide a scientific and effective approach to detecting and analyzing land cover changes (Roy and Saha 2016). The Digital Elevation Model (DEM) offers a strong technical foundation for developing digital hydrological models used in watershed extraction and topographic analysis (Mantelli et al. 2011). DEMs, which provide basic elevation data, are freely available from the ASTER (Advanced Spaceborne Thermal Emission and Reflection Radiometer) mission by Japan (Srivastava and Mondal 2012). Land use and land cover change detection involves identifying differences in an object or phenomenon by observing it at different time points (Panuju et al. 2020). These changes are driven by socioeconomic, political, cultural, demographic, and environmental conditions, often influenced by high population density (Briassoulis 2020). Remote sensing (RS) technology is one of the most effective tools for studying spatial and temporal changes in vegetation health. A decline in vegetation health and plant species diversity reduces soil erosion resistance and soil fertility (Berendse et al. 2015).

The Normalized Difference Vegetation Index (NDVI) is one of several spectral vegetation indices used to assess vegetation health (Pettorelli 2013). The NDVI technique is based on the principle that healthy vegetation exhibits low reflectance in the visible range of the electromagnetic spectrum due to chlorophyll content (Campbell 2002). Surface temperature is a key factor in determining the Earth's terrestrial thermal behavior, as it controls the effective radiating temperature of the land surface (Zhang et al. 2008). Retrieving surface temperature from remotely sensed thermal infrared (TIR) data, particularly from Landsat-8 TIR bands, has gained significant attention. Landsat-8 carries two sensors: the Operational Land Imager (OLI) and the Thermal Infrared Sensor (TIRS), while Landsat-5 Thematic Mapper (TM) has a spatial resolution of 120 meters (Reuter et al. 2011).

Kaptai lake has significantly altered the water levels and elevation of the sub-basin, led to land cover changes, substantially reduced vegetation health, and caused temperature changes over the past 42 years. To investigate these issues, it is essential to map the trends in water levels and land cover changes (1976-2018), as well as changes in vegetation health and surface temperature (1989-2018), in Kaptai lake and its surrounding areas using remote sensing technology and spatial analysis techniques in Geographic Information Systems (GIS). There has been no research into temporal land cover change pattern mapping using high-resolution satellite images in the Kaptai watershed. Most previous studies have relied on survey-based and laboratory-based experiments rather than remote sensing and data-driven approaches. Therefore, the aim of this study is to detect changes in water bodies and land cover between 1976 and 2018, changes in vegetation health from 1989 to 2018 and analyze the relationship between surface temperature variation and other environmental characteristics of the Kaptai sub-basin from 1989 to 2018.

Materials and methods

Study area

Kaptai lake (Map 1) is located primarily in the Rangamati district, with a portion extending into the Khagrachhari district. The Kaptai reservoir was created by constructing an earthen dam across the Karnaphuli river at Kaptai, approximately 70 km upstream from the estuary near Chattogram. The reservoir covers an area of about 58,300 hectares. Its maximum and average depths are 35 meters and 9 meters, respectively. The mean annual water level fluctuation is 8.14 meters, and the total water storage capacity is approximately 524.7×10^6 cubic meters (Ahmed and Mehner 2024).

Data collection and processing

We acquired multispectral and multi-temporal LANDSAT and ASTER satellite data for the Kaptai sub-basin covering a 42-year period from 1976 to 2018. All LANDSAT and ASTER images were obtained from the USGS Earth Explorer platform. The 1976 image is from Landsat 2 (MSS), while the 1989 and 2005 images are from Landsat 5 (TM), and the 2018 image is from Landsat 8 (OLI-TIRS), each with a spatial resolution of 30 meters. To delineate the study area, a DEM from the ASTER satellite (2011) with a 15-meter resolution was used. All satellite images were projected using the Universal Transverse Mercator (UTM) Zone 45N and the World Geodetic System 1984 (WGS-84) datum. Appendix 1 presents the list of data sources along with acquisition dates, resolutions, and sources.

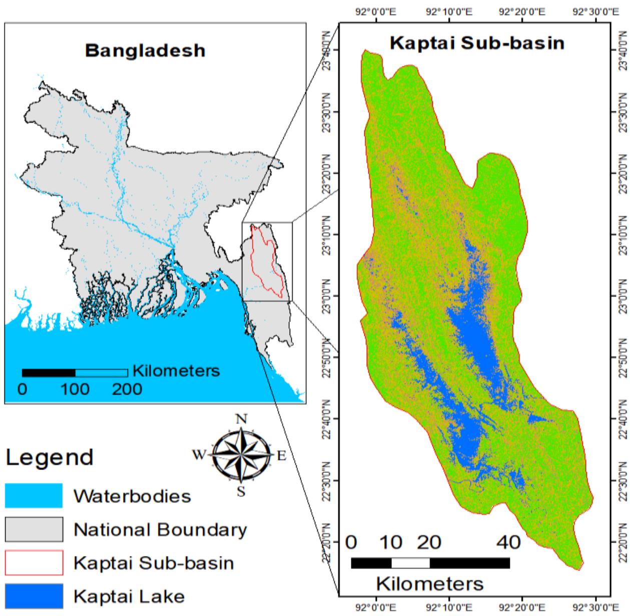

Map 1. Location of the study area

The Landsat images were obtained as "Level 1 data" from the USGS Earth Explorer website. Since the Landsat 2 MSS sensor lacks Band 4 (Near Infrared), Band 5 (Shortwave Infrared), and Bands 10 and 11 (Thermal Infrared), it cannot be used to estimate NDVI or surface temperature. Therefore, vegetation health and surface temperature in the Kaptai sub-basin were analyzed using Landsat 5 (Bands 4 and 5) and Landsat 8 (Bands 10 and 11) over the period from 1989 to 2018, covering 29 years.

All the satellite imagery was geo-referenced using the ground control points (GCPs) collected from the field using a standard GPS device. Three distinct GCPs were chosen for each image. The geometric error was checked for each image using the following equation:

$$RMSerror = \sqrt{(x' - xorig)^2 + (y' - yorig)^2}$$

Where, x' is latitude of the image, y' is longitude of the image, *xorig* is original latitude of the ground, and *yorig* is the original longitude of the ground. Appendix 2 shows the average root mean square error for each dataset.

Study area demarcation

The initial stage of data processing in this research was conducted using ArcGIS 10.5 to define the study area from the Digital Elevation Model (DEM). DEMs provide detailed terrain representation and are widely used in watershed modeling. In this study, an ASTER DEM with a spatial resolution of 30 meters, acquired on October 2, 2011, was used to cover the Kaptai sub-basin area. Four ASTER satellite images were mosaicked using ENVI Classic 5.3 software to create a seamless representation of the Kaptai watershed.

The DEM was constructed from a Triangulated Irregular Network (TIN) using the 3D Analyst tool in ArcMap. To simplify processing and ensure spatial accuracy, the image was clipped using map coordinates derived from the ASTER DEM. Before classification, the precise boundaries of the study area were digitized using the Region of Interest (ROI) tool in ENVI Classic 5.3 to create a mask band. This mask band allowed subsequent operations to be performed exclusively within the defined study area, reducing processing complexity and enhancing result accuracy.

Water level and land cover changes

Three land use/land cover (LULC) classes were established: vegetation, water bodies, and others (including buildings, concrete areas, and bare soil). The classified maps for the years 1976, 1989, 2005, and 2018 are presented in Map 2. ENVI Classic 5.3 supports both supervised and unsupervised image classification. In this study, the "Maximum Likelihood" algorithm under the supervised classification method was employed to achieve more accurate results.

The classification process was based on preselected ROI. Using Landsat band combinations Infrared (RGB: bands 4, 3, 2) and Natural Color (RGB: bands 7, 4, 2) along with field knowledge and personal observation, the study area was classified into three ROIs corresponding to the identified LULC classes.

Vegetation health monitoring using NDVI

To monitor vegetation health between 1989 and 2018, the Normalized Difference Vegetation Index (NDVI) was assessed. ENVI Classic 5.3 provides a built-in

NDVI tool that allows direct generation of NDVI maps. NDVI is calculated using the reflectance of visible and near-infrared (NIR) light from vegetation. Healthy vegetation absorbs most visible light and reflects a large portion of NIR light, whereas unhealthy or sparse vegetation reflects more visible light and less NIR light. NDVI is calculated using the following formula Arulbalaji and Gurugnanam (2014)-

$$NDVI = \frac{\text{NIR} - \text{VIS}}{\text{NIR} + \text{VIS}}$$

Where NIR refers to the spectral reflectance in the near-infrared band (0.725–1.1 µm), dominated by light scattering from the canopy, and VIS refers to the reflectance in the red (visible) band (0.58–0.68 µm), the portion of the spectrum most absorbed by chlorophyll. To observe the gradual change in vegetation health over time, it is essential to extract the NDVI histogram.

ENVI Classic 5.3 was used to generate NDVI maps for the years 1989 to 2018, and the corresponding NDVI histograms were extracted for analysis. The NDVI values range from -1 to +1, where increasing positive values indicate healthier and denser green vegetation, while negative values correspond to non-vegetated surface features such as water bodies, built-up areas, or bare soil.

Estimate surface temperature

ArcGIS 10.5 software was utilized to retrieve land surface temperature (LST) for the Kaptai sub-basin. The process involved several sequential steps using image processing tools within the software to generate both surface temperature and vegetation index maps. Initially, the digital number (DN) values from the satellite images were converted into top-of-atmosphere (TOA) radiance. This was followed by the calculation of TOA brightness temperature. Next, the NDVI was computed to assess vegetation health, which is crucial for estimating surface emissivity. Land surface emissivity (LSE) was then derived based on NDVI values. Using this information, LST was calculated. Finally, average surface temperature was determined using the cell statistics function. These procedures were applied to Landsat 5 TM and Landsat 8 OLI/TIRS satellite data to estimate the surface temperature of the Kaptai sub-basin over time.

Results and discussion

Land cover of Kaptai sub-basin for different times

Map 2 illustrates the land cover distribution of the Kaptai sub-basin for the years 1976, 1989, 2005, and 2018, highlighting three distinct land cover categories represented by different colors: "others" (including settlement areas, barren land, and non-vegetated areas) in red, water bodies in blue, and vegetation in green.

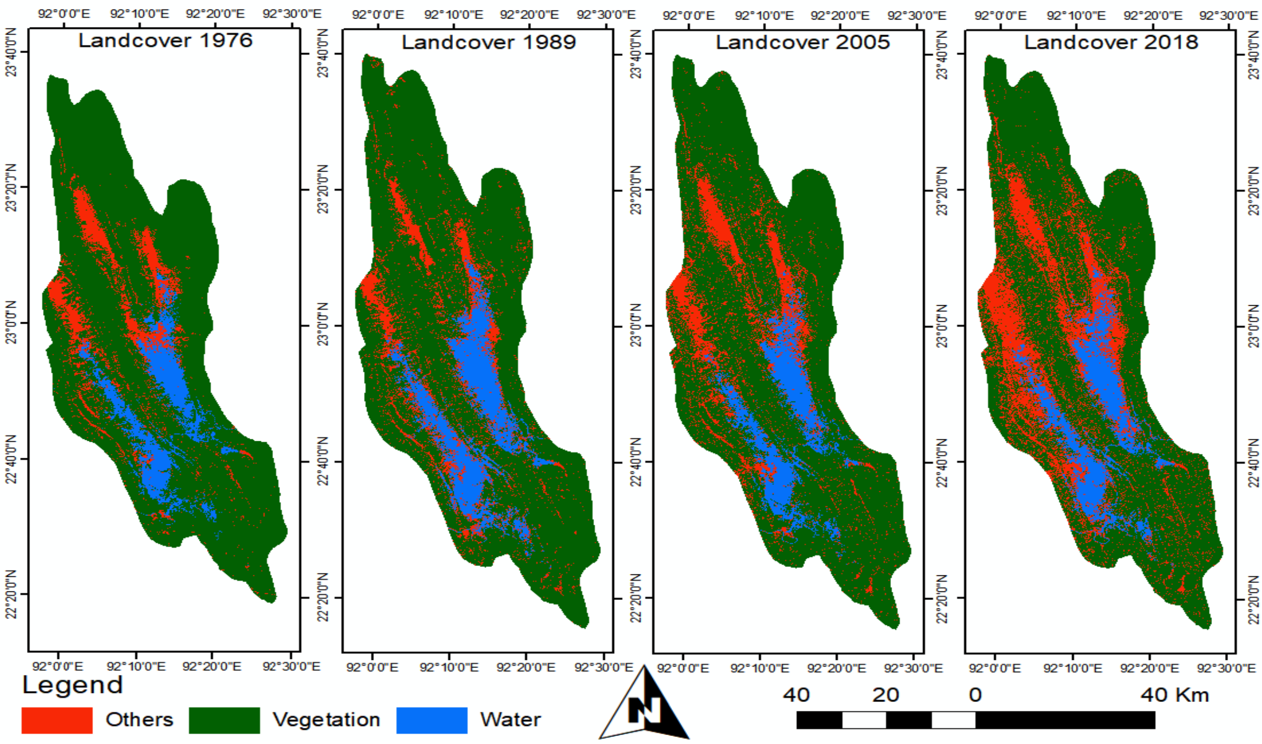

Map 2. Land cover of Kaptai sub-basin for 1976, 1989, 2005, and 2018

These maps were generated using the maximum likelihood classification method, and the corresponding statistical values are presented in Fig. 1. In the 1976 land cover map, the red-colored "others" category appears minimal, indicating limited settlement and human activity in and around Kaptai lake during that time. In contrast, vegetation (green) was the dominant land cover.

By 1989, the red area had slightly increased, as did the blue area representing water bodies, suggesting a modest expansion of settlements and water coverage, accompanied by a slight decrease in vegetation (Map 2). The land cover maps of 2005 and 2018 show a more pronounced increase in the red-colored areas compared to 1976 and 1989, indicating significant growth in settlements and non-vegetated land over time, with a corresponding decline in vegetative cover.

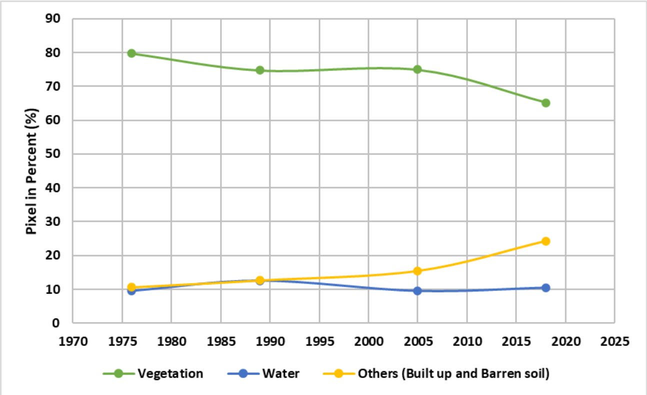

Fig. 1. Different land cover types of Kaptai sub-basin from 1976 to 2018

Figure 1 illustrates the change patterns of different land cover types in the Kaptai sub-basin from 1976 to 2018 using a line chart. The chart clearly shows a gradual decline in vegetation cover, while the "others" category, which includes built-up areas and barren soil, shows a steady increase, particularly in recent years. If current trends persist, increased human activities such as urbanization, soil erosion, landslides, and deforestation are likely to continue. This trend suggests that vegetation areas and water bodies are diminishing, while non-vegetative land cover types are expanding, indicating a steady degradation of the natural environment in the Kaptai sub-basin (Karmakar et al., 2011). Although the change in water levels in Kaptai lake is not highly significant, it is important to note that the lake's water level has been deliberately maintained to support hydroelectric power generation, navigation, freshwater supply, and tourism (Hoque et al. 2021).

Fig. 2a shows that in 1976, vegetation covered 803,487 pixels, accounting for approximately 79.80% of the total land cover in the Kaptai sub-basin. In contrast, water bodies and "others" (including settlements, concrete areas, and bare soil) occupied 96,201 pixels (10.48%) and 107,302 pixels (10.66%), respectively. These values indicate that vegetation was the dominant land cover type in the Kaptai sub-basin at that time. The data from subsequent study years- 1989, 2005, and 2018 reveal changes in the distribution of land cover types over time. A clear temporal trend is observed: the area covered by vegetation steadily decreases, while the area classified as "others" increases significantly. However, the change in water body coverage during the study period is relatively minor and less pronounced compared to the shifts in vegetation and other land cover types.

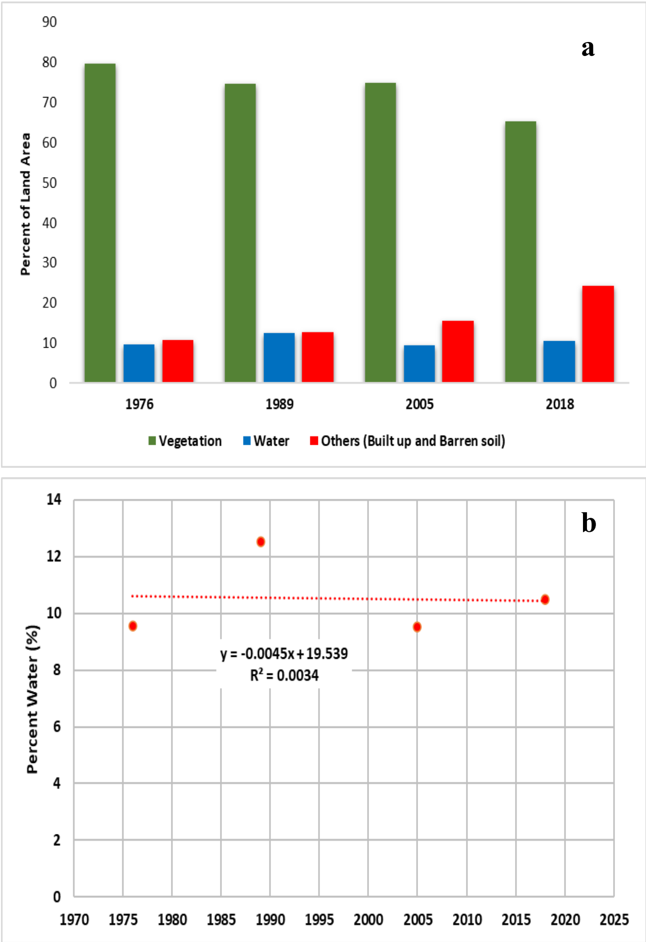

Fig. 2. (a) Land cover change pattern in 1976, 1989, 2005 & 2018; (b). Water level change pattern on temporal basis in the Kaptai sub-basin

Fig. 2b presents a comparison of land cover patterns across the selected time periods. The water body shows relatively stable coverage, while the vegetation cover exhibits a gradual decline, from approximately 80% to 65%. In contrast, the category labeled “others” (which includes built-up areas and barren soil) fluctuates, increasing from around 10% to 24%. Fig. 2b illustrates the water level change trend in Kaptai Lake from 1976 to the present, expressed using the regression coefficient (R^2). This statistical measure helps evaluate how well future outcomes can be predicted based on existing data. In this study, the R^2 value for water level change is 0.0034, significantly lower than 1, indicating an extremely weak trend over time. Such a low R^2 suggests that there has been minimal change in the lake's water level across the study period and that this pattern is likely to continue in the near future. However, despite this statistical stability, Kaptai lake is experiencing gradual reductions in water level due to environmental factors such as landslides, soil erosion from declining vegetation, and sedimentation (Tushar et al. 2024). These factors pose a growing threat to the natural balance of the Kaptai sub-basin (Tonni 2022).

Vegetation health monitoring of Kaptai sub-basin over time

Map 3 shows plant health maps for 1989, 2005, and 2018. It uses color-coded categories to show water bodies, paved surfaces, and different levels of vegetation health. Water bodies are expressed in blue, paved surfaces in pink. Vegetation health is shown across three classes: sparse vegetation (yellow), moderate vegetation (light green), and dense vegetation (dark green). These maps show how the health of the plants in the Kaptai sub-basin has worsened over time. The most concerning change is evident in the 2018 map, which shows a significant reduction in dense vegetation areas, now limited to only a small portion of the region. On the other hand, regions with little or moderate vegetation have become more dominant. This presents a clear pattern of vegetation loss and ecological stress in the Kaptai sub-basin (Ahammad 2019).

Fig. 3 presents the NDVI histogram results derived from ENVI Classic 5.3 for the years 1989, 2005, and 2018. These histograms illustrate the distribution of vegetation health in the Kaptai sub-basin based on NDVI values. Dense vegetation corresponds to NDVI values ranging from approximately 0.4 to 0.52, and its coverage, represented in green, declines noticeably over time. Moderate vegetation is associated with NDVI values between 0.3 and 0.4, while sparse vegetation falls within the NDVI range of 0.1 to 0.2, indicated by light green and yellow colors in the histogram. In 1989, the highest NDVI peak occurred at 0.6, indicating a dominance of dense vegetation in the region. By 2005, the peak shifted to 0.44, suggesting a reduction in dense vegetation and an increase in moderate vegetation cover. In 2018, the highest peak further declined to 0.31, signifying that moderate vegetation became the dominant category, with dense vegetation limited to a small portion of the sub-basin. These trends reflect a clear and gradual deterioration in vegetation health over the 29-year study period. The classification of vegetation health for each year, based on NDVI values, is summarized in Table 1.

Table 1. Vegetation health classification for Kaptai sub-basin from 1989 to 2018

Land cover classification	**Surface feature**	**NDVI value**	**Percent of pixel (%)**		
			1989	**2005**	**2018**
Non-vegetation class	Water	<0.1	15.66	14.62	13.02
	Paved surface	0.1-0.2	10.43	14.73	26.47
Vegetation health class	Sparse vegetation	0.2-0.3	13.04	14.67	19.32
	Moderate vegetation	0.3-0.4	13.04	14.68	19.83
	Dense vegetation	>0.4	47.83	41.3	21.36

In 1989, only 10.43% of the Kaptai sub-basin was covered by paved surfaces, which shows that human activity and settlement were still quite limited at that time. Most of the land was covered with vegetation, especially dense vegetation, which made up 47.83% of the area. Sparse and moderate vegetation together accounted for 13.04%, which means that the natural environment was still largely intact. However, by 2018, the situation had changed noticeably. Paved surfaces had increased to 26.47%, reflecting a significant rise in settlement and infrastructure development. At the same time, vegetation health had declined. Dense vegetation dropped to just 21.36%, while sparse and moderate vegetation rose to 19.32% and 19.83%, respectively. This shift indicates a clear reduction in healthy vegetation cover, which raises concerns for the region’s environment and wetland

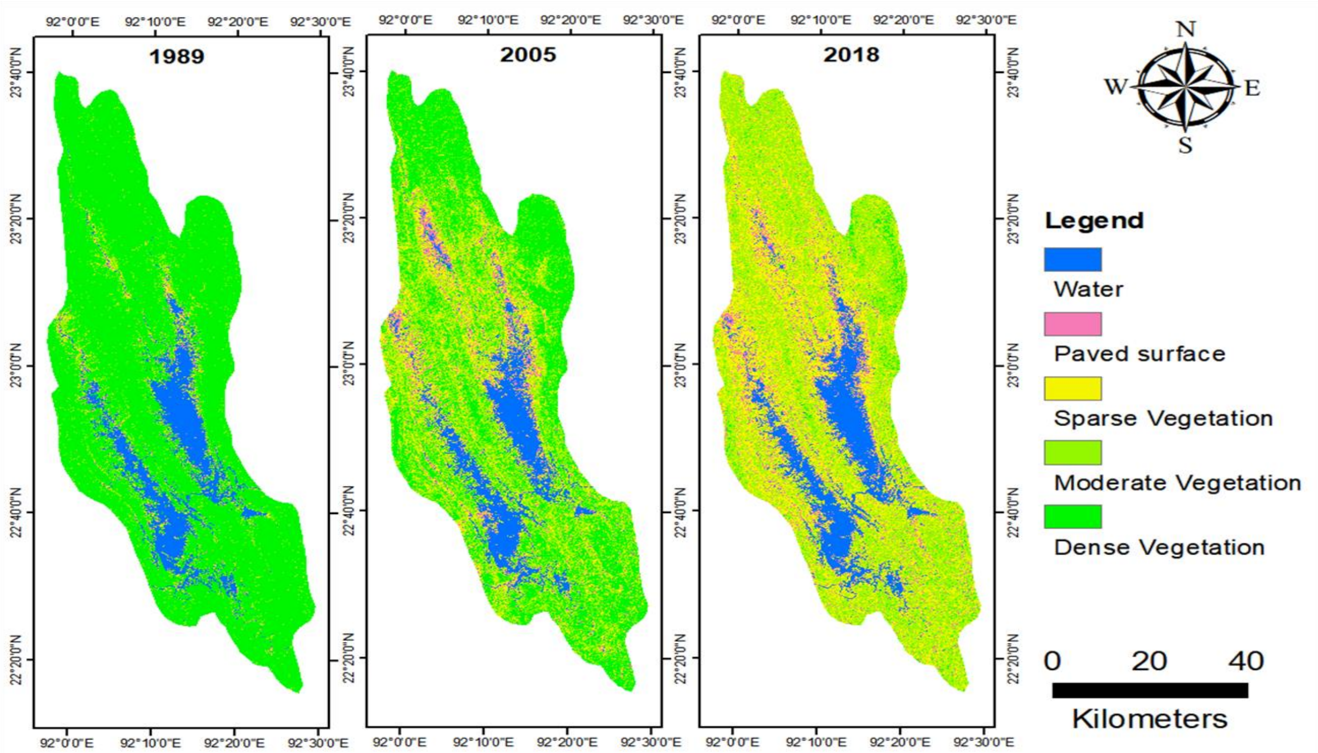

Map 3. Vegetation health classification map of 1989, 2005, and 2018 of Kaptai sub-basin

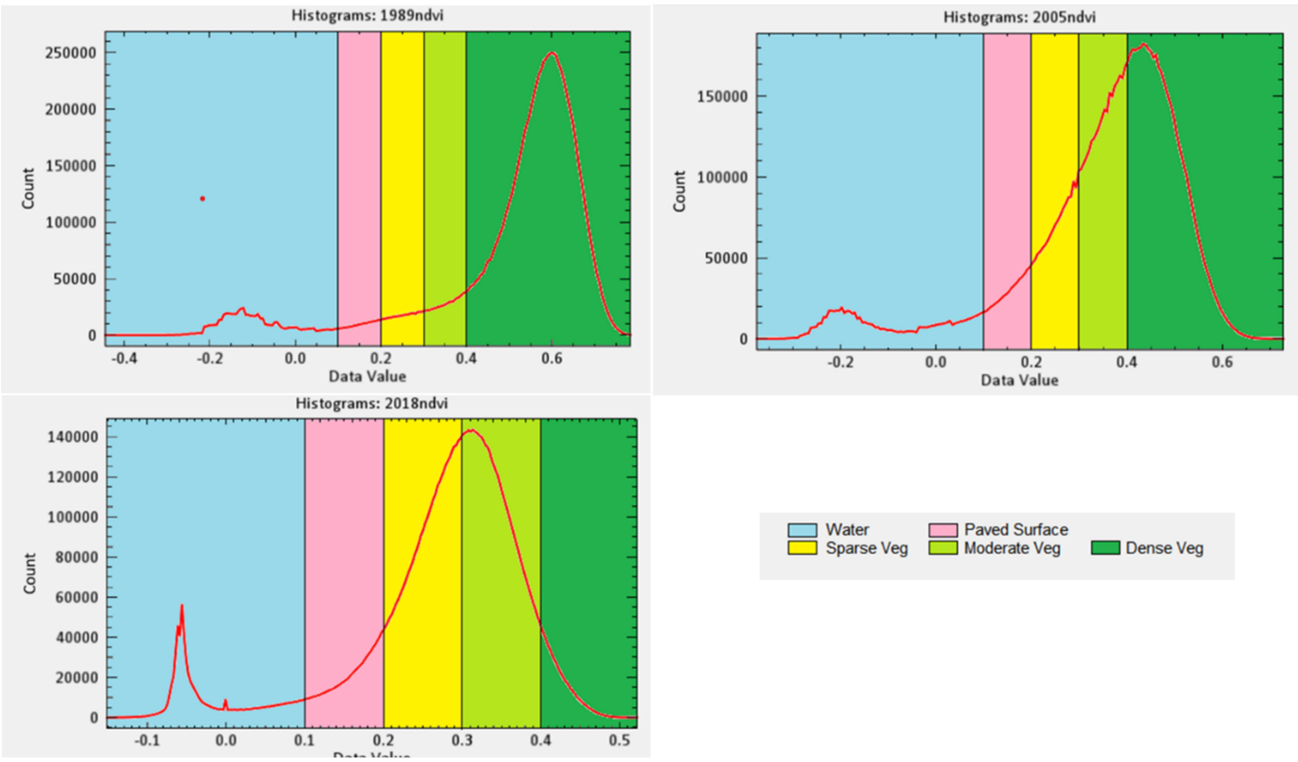

Fig. 3. NDVI histogram result from ENVI Classic 5.3 of 1989, 2005, and 2018

ecosystems (Table 1). Fig. 4 provides a quick look at how vegetation types changed over time. In 1989, vegetation covered about 74% of the area, 13% sparse, 13% moderate, and 48% dense. By 2005, vegetation cover dropped slightly to 70.65%, with 15% sparse, 15% moderate, and 41% dense vegetation. In 2018, vegetation cover declined even further to 60.51%, with 19% sparse, 20% moderate, and just 21% dense (Table

1). These changes highlight a steady decline in vegetation health over the years, mainly due to growing human activity in the Kaptai sub-basin.

Assessment of surface temperature over time in Kaptai sub-basin

In this study, surface temperature estimates for different years in the Kaptai sub-basin were taken during the same month, specifically, the last week of November in the winter season, to obtain accurate, clear, and cloud-free satellite images. Landsat 5 (TM) and Landsat 8 (OLI) satellite imagery were used for this purpose. This consistent timing ensures more reliable results, as surface temperatures vary significantly with the seasons. Using satellite images from different months could produce inconsistent temperature results. Map 4 shows the surface temperature distribution for the years 1989, 2005, and

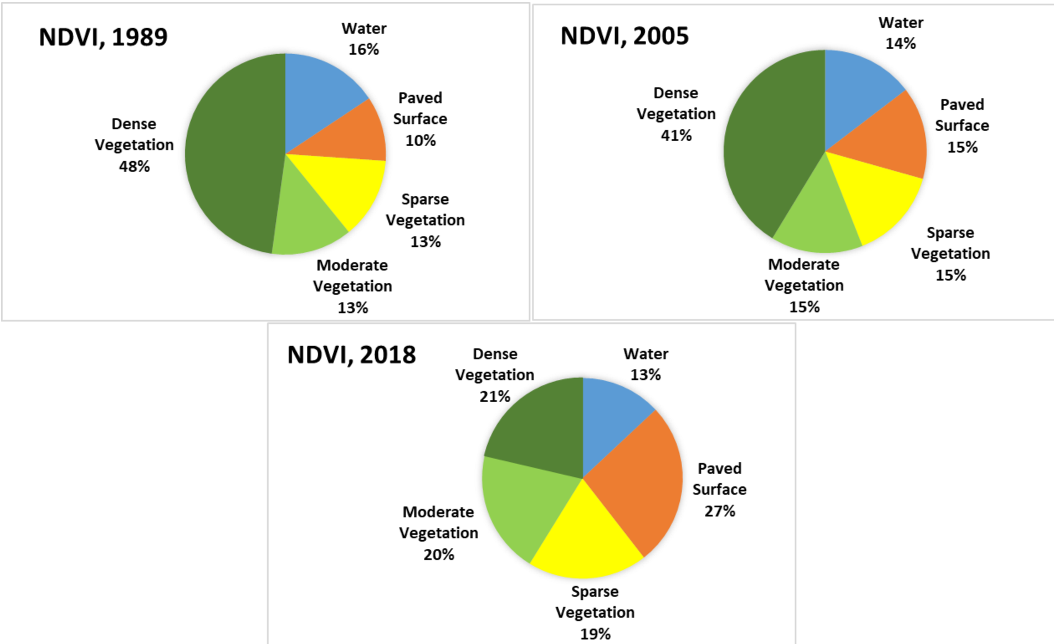

Fig. 4. Vegetation health classification from NDVI of 1989, 2005, and 2018

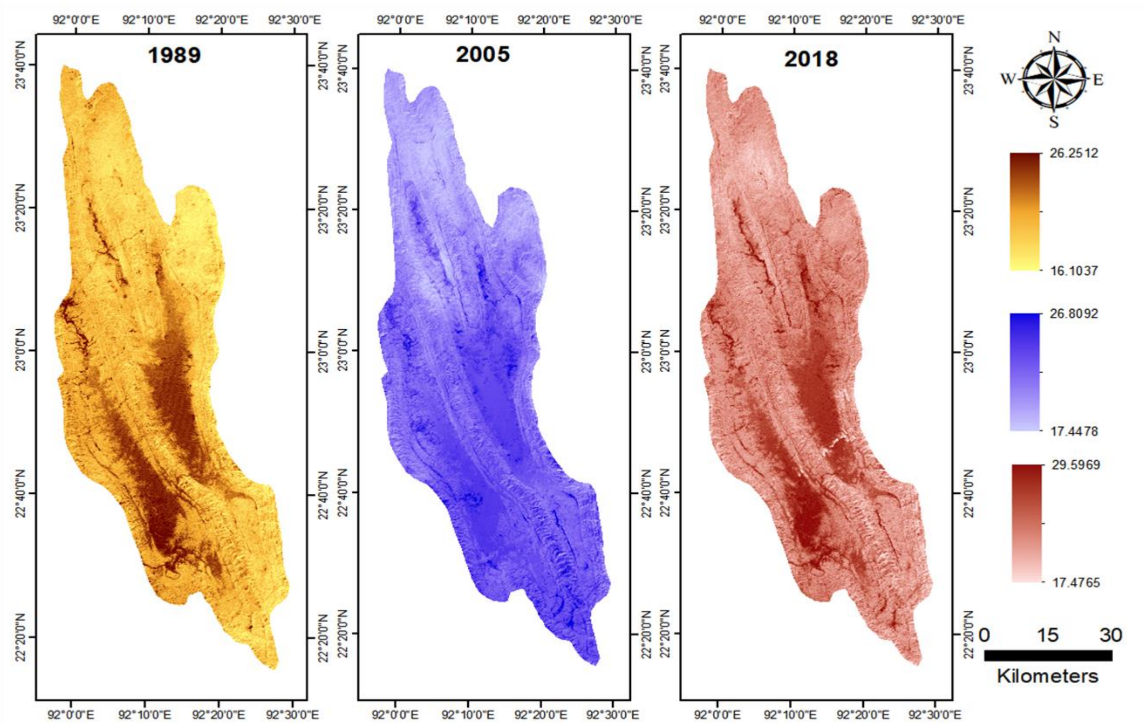

Map 4. Surface temperature map of 1989, 2005, and 2018 of Kaptai sub-basin Surface

2018 in the Kaptai sub-basin, with both maximum and minimum temperatures presented in degrees Celsius (°C), analyzed using ArcGIS 10.5. In these maps, deep shades of yellow, blue, and red indicate areas of higher surface temperature, typically representing water bodies, paved surfaces, built-up areas, and barren soil. Conversely, lighter shades of yellow, blue, and red represent cooler areas, usually associated with vegetation cover and forested regions of the Kaptai sub-basin.

Fig. 5 illustrates the changes in surface temperature within the study area for the years 1989, 2005, and 2018. In 1989, the maximum recorded temperature was 26.25°C, while the minimum was 16.10°C, reflecting relatively moderate temperatures largely associated with the extensive vegetation cover at that time. By 2018, the maximum temperature had risen to 29.60°C and the minimum to 17.48°C, indicating a noticeable increase in surface temperature over the 29 year period. This rise suggests a decline in vegetative cover and a corresponding increase in anthropogenic activities, including the expansion of paved surfaces such as concrete structures, built-up areas, and barren land, across the Kaptai sub-basin.

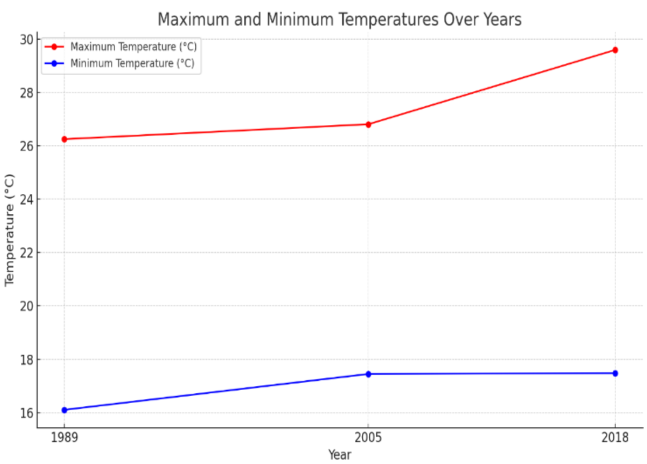

Fig. 5. Surface temperature change of Kaptai sub-basin

Fig. 6 shows the variation in surface temperature trends over time from 1989 to 2018. The changes in maximum temperature are noticeably higher in areas with paved surfaces, such as concrete structures, built-up areas, and barren soil, indicating a significant increase in these land cover types (Yahaya 2023). In contrast, the change in minimum temperature in vegetated areas is relatively minimal, suggesting a decline in vegetation cover over the study period (Jagtap et al. 2024).

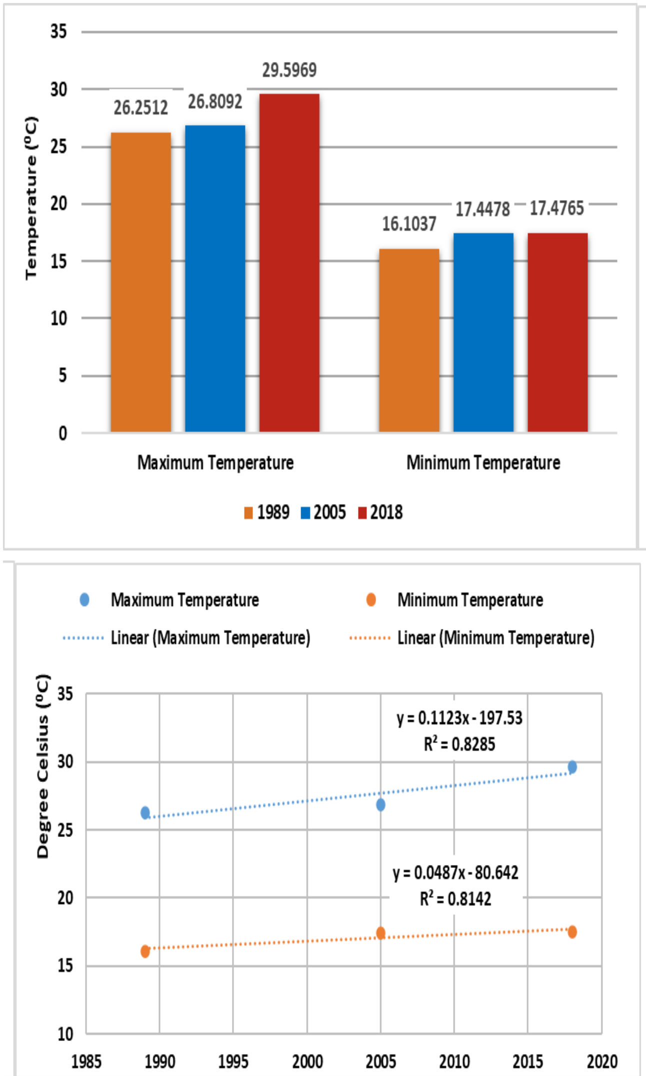

Fig. 6. Surface temperature change in 1989, 2005, and 2018

Trend of the surface temperature of the Kaptai sub-basin area

In this study, it was observed that there is a significant difference in the impact of using minimum versus maximum temperature values. The use of maximum temperature values increased the correlation, and the minimum values also showed a similar trend, with both contributing almost equally across all spectral ranges. As shown in Figure 6, the regression coefficient for maximum temperature is $R^2 = 0.8285$, while for minimum temperature is $R^2 = 0.8142$. Both values are close to 1, indicating a strong correlation and suggesting that the rate of surface temperature change is high in the present and is likely to continue in the near future if anthropogenic activities and human settlement persist (Rocha et al 2022).

Conclusion

The land cover analysis, vegetation health, and surface temperature in the Kaptai subbasin from 1976 to 2018 demonstrate considerable changes because of human activity. During this time, vegetation cover, mainly dense vegetation has continuously reduced, while settlements, built-up areas, and barren land have increased gradually. Vegetation of the landscape has changed from 80% in 1976 to 65% in 2018, with a significant shift toward moderate and sparse vegetation and a sharp increase in paved surfaces. Vegetation health, which was evaluated by NDVI values, demonstrates identical degradation. The dense vegetation percentage declined from 47.83% in 1989 to 21.36% in 2018, wherever paved surfaces increased twofold. Healthy vegetation declining is highly connected with increased urbanization, infrastructure development, and land use changes, which also cause the increase in the surface temperature at the same time. The maximum surface temperature in 1989 was 26.25°C, which increased to 29.60°C in 2018, with regression models showing a substantial rising trend that is likely to continue if existing land use patterns are maintained. Due to soil erosion, sedimentation, and landslides, the gradual water level reduction occurred; however, the water body coverage was relatively stable. The Kaptai sub-basin is currently facing significant environmental degradation, marked by the decline of healthy vegetation, the growth of built-up and non-vegetated regions, and increasing surface temperatures. Unplanned human activities, such as urbanization and land use changes, collectively degrade the ecological balance, wetland ecosystems, and the long-term sustainability of the study area. To minimize and conserve the sustainability of the environment, regular monitoring and proper management practices are necessary.

Acknowledgments

The authors would like to express their gratitude to the Environmental Science Discipline at Khulna University for providing access to the Geo-Informatics laboratory, which was essential for conducting this study as part of an M.Sc. (thesis) research.

References

Ahammad R (2019). Recent trends in forest and livelihood relationships of rural communities in the Chittagong Hill Tracts region, Bangladesh. PhD dissertation, Charles Darwin University. https://doi.org/10.25913/5e4f60e93cb55

Ahmed KKU & Mehner T (2024). Long-term records of fisheries yield and stocking in Kaptai reservoir (Bangladesh). Open Access Library Journal, 11, e12682.

Antonić O, Hatic D, Krian J & Bukovec D (2001). Modelling groundwater regime acceptable for the forest survival after the building of the hydro-electric power plant. Ecological Modelling, 138, 277-288. https://doi.org/10.1016/S0304-3800(00)00408-7

Arulbalaji P & Gurugnanam B (2014). Evaluating the normalized difference vegetation index using landsat data by ENVI in salem district, Tamilnadu, India. International Journal of Development research, 4(9), 1844-1846.

Berendse F, Ruijven J, Jongejans E & Keesstra SD (2015). Loss of plant species diversity reduces soil erosion resistance of embankments that are crucial for the safety of human societies in low-lying areas. Ecosystems, 1, 881–888.

Briassoulis H (2020). Analysis of Land Use Change: Theoretical and Modeling Approaches. 2nd edn. Regional Research Institute, West Virginia University, USA.

Campbell JB (2002). Introduction to remote sensing. CRC Press.

Dale VH, Efroymson RA & Kline KL (2011). The land use–climate change–energy nexus. Landscape Ecology, 26, 755-773. https://doi.org/10.1007/s10980-011-9606-2

Das B, Islam MA, Tamim U, Ahmed FT & Hossen MB (2024). Heavy metal analysis of water and sediments of the Kaptai Lake in Bangladesh: Contamination and concomitant health risk assessment. Applied Radiation and Isotopes, 210, 111358.

Hoque ME, Islam M, Karmakar S, Rahman MA & Bhuyan MS (2021). Sediment organic matter and physicochemical properties of a multipurpose artificial lake to assess catchment land use: a case study of Kaptai Lake, Bangladesh. Environmental Challenges, 3, 100070.

Jagtap AA, Shedge DK & Mane PB (2024). Exploring the effects of land use/land cover (LULC) modifications and land surface temperature

(LST) in Pune, Maharashtra with anticipated LULC for 2030. International Journal of Geoinformatics, 20(2), 42-63.

Karmakar S, Haque SSM, Hossain MM & Shafiq M (2011). Water quality of Kaptai reservoir in Chittagong Hill tracts of Bangladesh. Journal of Forestry Research, 22, 87-92.

Li L & Hao ZC (2003). The automated extraction of catchment properties from digital elevation models. Advances in Earth Science, 18, 251-256.

Mantelli LR, Barbosa JM & Bitencourt MD (2011). Assessing ecological risk through automated drainage extraction and watershed delineation. Ecological Informatics, 6, 325-331.

Panuju DR, Paull DJ & Griffin AL (2020). Change detection techniques based on multispectral images for investigating land cover dynamics. Remote Sensing, 12(11), 1781.

Pettorelli N (2013). The normalized difference vegetation index. Oxford University Press, USA.

Reuter D, Irons J, Lunsford A, Montanaro M, Pellerano F, Richardson C, Smith R, Tesfaye Z & Thome K (2011). The operational land imager (OLI) and the thermal infrared sensor (TIRS) on the Landsat data continuity mission (LDCM). In: Algorithms and technologies for multispectral, hyperspectral, and ultraspectral imagery XVII, 8048, 382-388. SPIE.

Rocha J, Oliveira S, Viana CM & Ribeiro AI (2022). Climate change and its impacts on health, environment and economy. In: One Health. Academic Press, 253-279 pp.

Roy B & Saha P (2016). Temporal Analysis of Land Use Pattern Changes in Chittagong District of Bangladesh using Google Earth and ArcGIS. Annual International Conference on Chemical Processes, Ecology & Environmental Engineering (ICCPEE'16) April 28-29, 2016 Pattaya (Thailand). 40-45 pp.

Salehin MU (2024). Overview of the Hydropower Perspective of Bangladesh. Overview of the Hydropower Perspective of Bangladesh. https://dx.doi.org/10.2139/ssrn.4709543

Seyam MMH, Haque MR & Rahman MM (2023). Identifying the land use land cover (LULC) changes using remote sensing and GIS approach: A case study at Bhaluka in Mymensingh, Bangladesh. Case Studies in Chemical and Environmental Engineering, 7, 100293.

Srivastava VK & Mondal K (2012). Evaluation of Digital Elevation Models (DEMs) generated from ASTER and SRTM data: A case study of flat alluvium terrain of Bakeshwar Fujisada, H. 1994. Overview of ASTER instrument on EOS-AM1 platform. Proceedings of SPIE, 2268, 14-36.

Suman KH, Hossain M, Salam MA, Rupok QSS & Haque MN (2021). Production trends, and challenges for biodiversity conservation and sustainable fisheries management of Kaptai lake, the largest reservoir in Bangladesh. Asian Fisheries Science, 34(2), 145-158.

Tonni ZF (2022). Quality assessment of the rain water sample collected from coastal territory and different location of Chattogram city. Doctoral dissertation, Chattogram Veterinary & Animal Sciences University, Bangladesh.

Tripura R (2021). Exploring Integrated Ecosystem-based Approach (EbA) in Kaptai lake Freshwater Fish Biodiversity, Rangamati, Bangladesh. Doctoral dissertation, Asian University for Women, Bangladesh.

Tushar MAN, Hossain A, Hossen M, Ahmed ME & Mia MB (2024). Spatiotemporal Assessment of Water Quality and Quantity of the Kaptai Lake at Rangamati, Bangladesh-An Approach of Remote Sensing, Field Investigation and Laboratory Analysis. The Dhaka University Journal of Earth and Environmental Sciences, 13(1), 121-139.

Yahaya AA (2023). Impact of vegetal cover loss on urban temperature and thermal comfort of residents in Abuja, Nigeria. Doctoral dissertation, Federal University of Technology, Minna, Niger State, Nigeria.

Zhang R, Tian J, Su H, Sun X, Chen S & Xia J (2008). Two improvements of an operational two-layer model for terrestrial surface heat flux retrieval. Sensors, 8(10), 6165-6187.

How to cite this article: Al-Amin M, Rahman MM, Nahar K, Islam R, Imam A, & Haque MK (2025). Temporal Land Use Change Pattern of Kaptai Lake and Surrounding Area Using Remotely Sensed Data. Aquatic Resource Sciences, 02, 01-12.

Appendix 1. Different satellite data used in this study from the Earth Explorer, USGS on June18, 2019

Data type & ID	Study type	Year	Scale (m)
ASTER	DEM for Study area	2011	15
Landsat 2 (MSS)	Water level and land cover change	1976	60
Landsat 5 (TM)	Water level and land cover change; NDVI and Surface temperature	1989, 2005	30
Landsat 8 (OLI-TIRS)	Water level and land cover change; NDVI and Surface temperature	2018	30

Appendix 2. RMS error during geo-referencing

Sl. No.	Corresponding year of image	RMS error in acquired data
1	1976	0.176985
2	1989	0.002271
3	2005	0.00155
4	2018	0.000085